Displacement and Polarization Switching Properties of Piezoelectric Laminated Actuators under Bending

doi: 10.1063/1.1603963

Displacement and polarization switching properties of piezoelectric laminated actuators under bending

Keisuke Hayashi, Yasuhide Shindo,[a] and Fumio Narita
Department of Materials Processing, Graduate School of Engineering, Tohoku University, Aoba-yama 02, Sendai 980-8579, Japan

(Received 14 April 2003; accepted 6 July 2003)

The displacement and polarization switching properties of piezoelectric laminated actuators have been investigated theoretically, numerically, and experimentally. A laminated beam theory solution is developed for the piezoceramic/metal/piezoceramic actuator, and the effects of electric fields on the displacements of the actuators are analyzed. The mathematical procedure of the present analysis is simple and clear, and the resulting solutions for the displacement of the cantilever laminated beam actuator are highly accurate. A nonlinear three-dimensional finite element analysis is also employed. Bending tests are used to validate the numerical predictions, using laminated actuators made with ferroelectric lead zirconate titanate piezoelectric layers and Fe-48% Ni host material. Good agreement is obtained between the tests and predictions. © *2003 American Institute of Physics.* [DOI: 10.1063/1.1603963]

I. INTRODUCTION

In recent years, considerable effort has been focused on the development of active sensing and reactive smart structures. The coupled electromechanical properties of piezoelectric ceramics make them well suited for use as sensors and actuators in smart devices and structures. Piezoelectric layers are usually bonded to the surfaces of the host structure. To incorporate piezoelectric layers into a structure and to design high performance piezoelectric laminated actuators, an understanding of electromechanical interaction between the piezoelectric layers and the host structure is of great importance. Donthireddy and Chandrashekhara[1] developed a mathematical model for laminated composite beams with piezoelectric layers based on a layerwise theory. Wise[2] measured the electromechanical displacement properties of piezoelectric actuators. Li *et al.*[3] examined the static and dynamic electromechanical response of piezoelectric–nonpiezoelectric unimorphs with various thickness ratios and shapes. Vel and Batra[4] obtained an exact state space solution for the three-dimensional (3D) cylindrical bending deformations of laminates with embedded piezoelectric shear actuators.

The aforementioned studies deal with linear piezoelectric actuators. In some practical structures, one major concern has been the polarization switching of the piezoelectric ceramic layers. In this article, we present theoretical, numerical, and experimental results on the nonlinear displacement properties of piezoelectric laminated actuators. The electroelastic response of piezoceramic/metal/piezoceramic actuator is analyzed based on the laminated beam theory. A nonlinear finite element model is also used, and the effects of external electrical loading, geometric shape, and material properties on the displacement of the cantilever piezoelectric laminated actuators are examined. It is shown that nonlinear material behavior is induced by polarization switching. In order to confirm the numerical results, bending tests on the cantilever actuator are performed, and the electromechanical displacement is measured. Results produced by the model are compared with experimental values. This comparison indicates good agreement between the model prediction and test data.

II. ELECTROELASTIC ANALYSIS

A. Basic equations and polarization switching criterion

Mechanical equilibrium and Gauss' law are given by

$$\sigma_{ji,j}=0, \tag{1}$$

$$D_{i,i}=0, \tag{2}$$

where σ_{ij} and D_i are the stress and electric displacement, and a comma followed by an index denotes partial differentiation with respect to a space coordinate $x_i(i=1,2,3)$. We have employed Cartesian tensor notation and the summation convention for repeated tensor indices. Constitutive equations are

$$\varepsilon_{ij}=s_{ijkl}\sigma_{kl}+d_{kij}E_k, \tag{3}$$

$$D_i=d_{ikl}\sigma_{kl}+\epsilon_{ik}E_k, \tag{4}$$

where ε_{ij} and E_i are the strain and electric field, and s_{ijkl}, d_{kij}, and ϵ_{ik} are the elastic compliance, direct piezoelectric, and dielectric constants, which satisfy the following symmetry relations:

$$s_{ijkl}=s_{jikl}=s_{ijlk}=s_{jilk}=s_{klij}, \quad d_{kij}=d_{kji}, \quad \epsilon_{ij}=\epsilon_{ji}. \tag{5}$$

The strain and electric field are

$$\varepsilon_{ij}=\tfrac{1}{2}(u_{j,i}+u_{i,j}), \tag{6}$$

$$E_i=-\phi_{,i}, \tag{7}$$

[a]Electronic mail: shindo@material.tohoku.ac.jp

where u_i and ϕ are the displacement and electric potential, respectively. The constitutive Eqs. (3) and (4) for ferroelectric lead zirconate titanate (PZT) poled in the x_3 direction are found in the Appendix.

When a high electric field is applied to the piezoelectric ceramic layer, polarization switching occurs. The polarization of each grain aligns as closely as possible with the electric-field direction, and the remanent polarization and strain develop. The criterion requires that a polarization switches when the combined electrical and mechanical work exceeds a critical value[5]

$$\sigma_{ij}\Delta\varepsilon_{ij}+E_i\Delta P_i \geqslant 2P^s E_c, \tag{8}$$

where $\Delta\varepsilon_{ij}$ and ΔP_i are the changes in the spontaneous strain and polarization during switching, respectively, P^s is a spontaneous polarization, and E_c is a coercive electric field. The constitutive Eqs. (3) and (4) during polarization switching are

$$\varepsilon_{ij}=s_{ijkl}\sigma_{kl}+d'_{kij}E_k+\varepsilon^r_{ij}, \tag{9}$$

$$D_i=d'_{ikl}\sigma_{kl}+\varepsilon_{ij}E_k+P^r_i, \tag{10}$$

where ϵ^r_{ij} and P^r_i are the macroscopic remanent strain and polarization, respectively. The value of direct piezoelectric constant d'_{ikl} of each grain is[6]

$$d'_{ikl}=d_{33}n_in_kn_l+d_{31}(n_i\delta_{il}-n_in_kn_l) + \tfrac{1}{2}d_{15}(\delta_{ik}n_l-2n_in_kn_l+\delta_{il}n_k), \tag{11}$$

where n_i is the unit vector in the polarization direction and δ_{ij} is the Kronekr delta. The values of $\Delta\varepsilon_{kl}$ and ΔP_i are given here for polarization switching in the x_1x_3 plane with x_3 as the original poling direction. The changes in spontaneous strain $\Delta\varepsilon_{kl}$ and polarization ΔP_i for 180° switching can be expressed as

$$\Delta\varepsilon_{11}=0,\quad \Delta\varepsilon_{22}=0,\quad \Delta\varepsilon_{33}=0,\quad \Delta\varepsilon_{12}=0,$$
$$\Delta\varepsilon_{23}=0,\quad \Delta\varepsilon_{31}=0,$$
$$\Delta P_1=0,\quad \Delta P_2=0,\quad \Delta P_3=-2P^s. \tag{12}$$

For 90° switching in the x_1x_3 plane,

$$\Delta\varepsilon_{11}=\gamma^s,\quad \Delta\varepsilon_{22}=0,\quad \Delta\varepsilon_{33}=-\gamma^s,$$
$$\Delta\varepsilon_{12}=0,\quad \Delta\varepsilon_{23}=0,\quad \Delta\varepsilon_{31}=0,$$
$$\Delta P_1=\pm P^s,\quad \Delta P_2=0,\quad \Delta P_3=-P^s, \tag{13}$$

where γ^s is the spontaneous strain.

B. Laminated beam theory

A laminated beam with integrated piezoelectric layers is shown in Fig. 1. Let the coordinate axes $x=x_1$ and $y=x_2$ be chosen such that they coincide with the middle plane of the laminated actuator and the $z=x_3$ axis is perpendicular to this plane. The host material chosen is a metal. PZT layers poled in the z direction are added to the upper and lower surfaces to make a three-layered piezoelectric actuator. The total thickness is $2h$ and the kth layer has thickness $h_k=z_k-z_{k-1}$ $(k=1,2,3)$ where $z_0=-h$ and $z_3=h$. For the present laminated beam theory, it is assumed that the electric field resulting from variations in stress (the so-called direct piezoelectric effect) is insignificant compared with the applied electric field.[7,8]

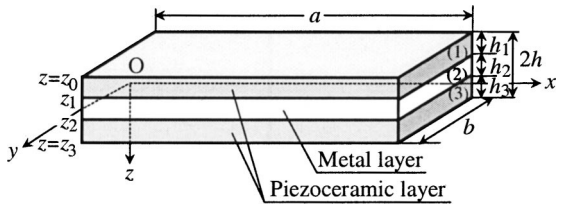

FIG. 1. Piezoelectric–metal–piezoelectric actuator.

In a piezoelectric laminated beam, the layers are free to expand vertically, which implies that the stress $(\sigma_{zz})_k$ is equal to zero. Also, because the beams are considered to be long and slender, we may assume that the stress $(\sigma_{yy})_k$ is zero. As the polarization is not perpendicular to the electric field $(E_z)_k$, no shear stresses will develop, and we may conclude that no shear strains are present, which will reduce the nontrivial stresses to $(\sigma_{xx})_k$. Considering the electric field inducing 180° switch, the lamina constitutive equation for the kth layer with respect to the reference axes of the laminate (x,z) can be expressed as

$$(\sigma_{xx})_k=\frac{1}{(s_{11})_k}(\varepsilon_{xx})_k-\frac{(d_{31})_k}{(s_{11})_k}(E_z)_k, \tag{14}$$

where

$$(s_{11})_k=s_{11}\quad (k=1,3),\quad (s_{11})_2=s^E_{11}, \tag{15}$$

$$(d_{31})_k=\begin{cases} d_{31} & (E_z>-E_c)\\ -d_{31} & (E_z\leqslant -E_c)\end{cases}\quad (k=1,3), \tag{16}$$

$$(d_{31})_2=0, \tag{17}$$

and s^E_{11} is an elastic compliance of the metal. The bending modulus per unit length, D, of the piezoelectric laminated actuator can be written as

$$D=\sum_{k=1}^{3}\int_{z_{k-1}}^{z_k}\frac{1}{(s_{11})_k}z^2dz. \tag{18}$$

The bending moment per unit length M^E_{xx} is given by

$$M^E_{xx}=\sum_{k=1}^{3}\int_{z_{k-1}}^{z_k}\frac{(d_{31})_k}{(s_{11})_k}(E_z)_k z\,dz. \tag{19}$$

C. Displacement of cantilever laminated beam actuator under electrical loading

Consider the electroelastic response of a cantilever piezoelectric laminated beam that is fixed at one end $(x=0)$ and subjected to an external electric field E_z. The differential equation for the displacement w can be expressed as

$$w_{,xx}=-\frac{M^E_{xx}}{D}. \tag{20}$$

The boundary conditions are given by

$$w=0,\quad w_{,x}=0\quad (x=0). \tag{21}$$

The solution for Eq. (20) is obtained as

TABLE I. Material properties.

	Elastic stiffnesses ($\times 10^{-12}$ m^2/V)				Piezoelectric coefficients ($\times 10^{-12}$ m/V)			Dielectric constants ($\times 10^{-10}$ C/Vm)	
	s_{11}	s_{33}	s_{44}	s_{13}	d_{31}	d_{33}	d_{15}	ε_{11}	ε_{33}
P-7B	16.7	18.8	38.8	−7.5	−303	603	592	418	283
P-7	15.8	18.1	40.6	−7.0	−207	410	550	171	186
N-10	14.8	18.1	44.9	−5.8	−287	635	930	443	481

$$w=-\frac{M_{xx}^{E}}{2D}x^2 \quad (0\leqslant x\leqslant a). \tag{22}$$

III. FINITE ELEMENT ANALYSIS

We performed 3D finite element calculations to determine the displacement for the cantilever laminated actuators. We use the commercial finite element code ANSYS. Eight-node 3D space solid was used in the analysis. The switching criterion of Eq. (8) is checked for every element and for every possible polarization direction to see if switching will occur. After all possible polarization switches have occurred, the direct piezoelectric constants of each element are changed. The spontaneous polarization P^s and strain γ^s are assigned representative values of 0.3 C/m^2 and 0.004, respectively.

IV. EXPERIMENTAL PROCEDURE

The present piezoelectric–metal–piezoelectric actuator was made of PZT and steel (Murata Manufacturing Co., Ltd., Japan). The piezoelectric PZT (P-7B) of thickness $h_p=0.2$ mm had silver paste electrodes on both sides. The steel layer of thickness $h_e=0.2$ mm was steel sheet (alloy, Fe-48% Ni). The material properties of P-7B are listed in Table I and the coercive electric field E_c is approximately 0.5 MV/m. The elastic compliance s_{11}^{E} and Poisson's ratio ν^E of Fe-48% Ni are taken to be $s_{11}^{E}=4.76\times10^{-12}$ m^2/N and $\nu^E=0.3$. The specimen had a length, a, of 43 mm, a width, b, of 2 mm, and a thickness, $2h=2h_p+h_e$, of 0.6 mm.

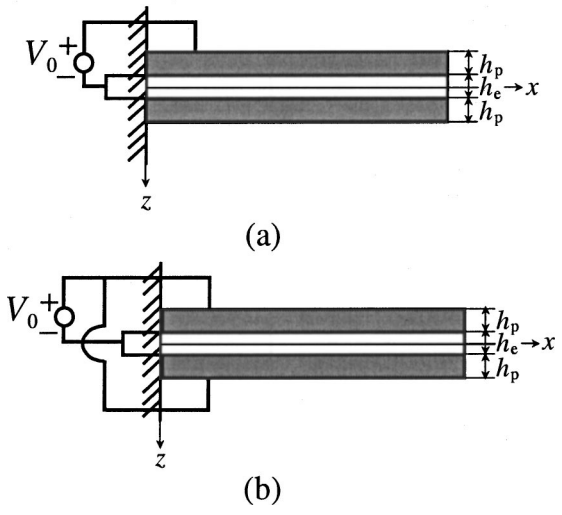

FIG. 2. Experimental setup: (a) unimorph and (b) bimorph.

The static displacements of the cantilever actuators were measured with a microscope, and the displacement under the applied voltage was recorded. The experimental setups are schematically shown in Figs. 2(a) and 2(b). First, a voltage V_0 was applied as shown in Fig. 2(a). The applied electric field E_0 is equal to the voltage V_0 divided by the distance h_p between the electrodes. Next, the same voltages were applied to the two piezoelectric layers. Referring to Fig. 2(b), we can identify the upper and lower piezoelectric layers, the upper with its polarization parallel and the lower having its polarization antiparallel to the electric field E_z. The bending moments for types a and b are $M_{xx}^{E}=(d_{31}/s_{11})V_0h_p$ and $2(d_{31}/s_{11})V_0h_p$, respectively. The resulting bending, all other parameters held constant, in a type b actuator is twice that of type a.

V. RESULTS AND DISCUSSION

We presented analytical and experimental results for a P-7B/Fe-48% Ni/P-7B actuator. The length, width, and thickness of the actuator are $a=43$ mm, $b=2$ mm, and $2h=0.6$ mm, respectively. Figure 3 gives a plot of the tip deflection w_{tip} with the applied electric field E_0 for $(E_z)_1=E_0=V_0/h_p$ and $(E_z)_3=0$ V/m (type a) showing the theoretical and numerical solutions and the experimental data for P-7B/Fe-48% Ni/P-7B actuator of $h_p=h_e=0.2$ mm. The tip deflection rises at first when the electric field E_0 is reduced starting at zero. As the electric field E_0 continues to be reduced, polarization switching commences at approximately $E_0=-0.4$ MV/m and since the remanent polarization is now diminishing, the tip deflection w_{tip} falls. Simultaneously, the piezoelectric effect of the upper layer is degraded and when the electric field reaches approximately -0.5 MV/m and the

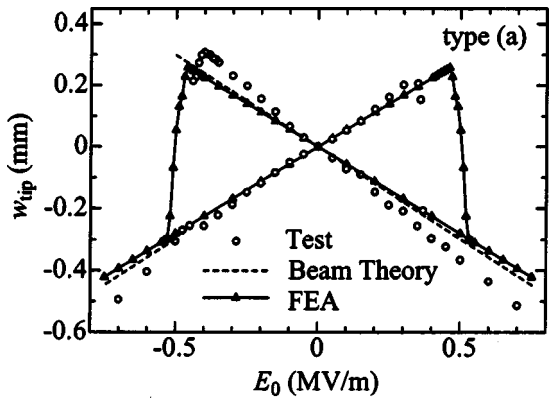

FIG. 3. Tip deflection vs electric field [P-7B, $h_p=h_e=0.2$ mm, $(E_z)_1=E_0$, and $(E_z)_3=0$].

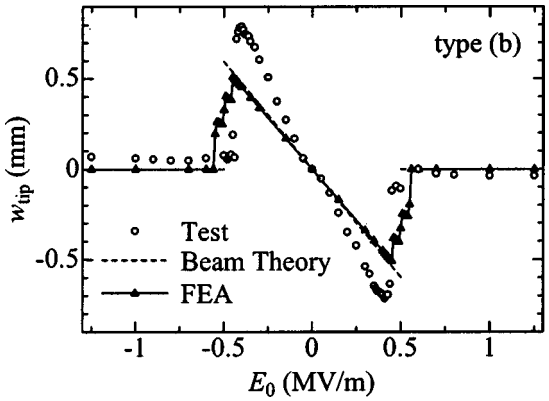

FIG. 4. Tip deflection vs electric field [P-7B, $h_p = h_e = 0.2$ mm, and $(E_z)_1 = -(E_z)_3 = E_0$].

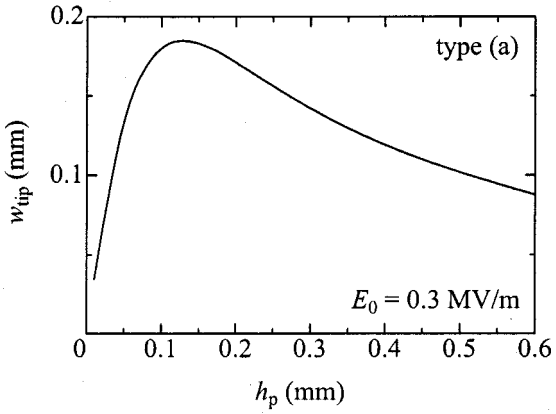

FIG. 6. Tip deflection vs piezoelectric layer thickness [P-7B, $h_e = 0.2$ mm, $(E_z)_1 = E_0$, and $(E_z)_3 = 0$].

remanent polarization of the upper layer is zero, the tip deflection w_{tip} has reached zero as well. However, as the field is reduced below -0.5 MV/m, a negative remanent polarization develops in the upper layer and the tip deflection w_{tip} is rebuilt. Look up now occurs as the electric field is brought toward approximately -0.55 MV/m. After this value is reached, switching is halted and the response is linear. The electric field in the z direction is now increased again toward 0.5 MV/m. Numerical results show that switching recommences at approximately $E_0 = 0.45$ MV/m to eliminate the existing negative remanent polarization. This is completed by the time the field reaches approximately 0.5 MV/m at which stage the tip deflection w_{tip} once again goes to zero. As the field is cycled between approximately -0.55 MV/m and 0.55 MV/m, the initial butterfly loop is repeated. The trend is sufficiently similar between the analyses and experiment. Figure 4 displays the tip deflection w_{tip} versus applied electric field E_0 for $(E_z)_1 = -(E_z)_3 = E_0 = V_0/h_p$ (type b) showing the analytical and experimental data for P-7B/Fe-48% Ni/P-7B of $h_p = h_e = 0.2$ mm. The curve rises steeply at first when the electric field E_0 is reduced starting at zero. Switching causes in the upper layer after the field is reduced to about -0.4 MV/m, and the magnitude of tip deflection diminishes until it disappears when the E_0 is equal to about -0.55 MV/m. As the electric field E_0 is increased from zero, the negative tip deflection is increased. After E_0 reaches about 0.4 MV/m, polarization switching of the lower layer can cause a decrease in the negative deflection, and the deflection returns to zero.

Next, the effects of geometric shape and material properties on the maximum displacement of the PZT/metal/PZT actuator under $(E_z)_1 = E_0$ and $(E_z)_3 = 0$ V/m (type a) are discussed. Thickness $2h$ is varied while keeping the length and width fixed at $a = 43$ mm and $b = 2$ mm, respectively. P-7B, P-7 (Refs. 9 and 10), and N-10 (NEC/Tokin Co., Ltd., Japan) ceramics properties as given in Table I are used for the numerical examples. The coercive electric fields of P-7 and N-10 are approximately 0.8 and 0.36 MV/m, respectively. Figure 5 shows the variation of the tip deflection w_{tip} of the finite element solutions with E_0 for the type a P-7B/Fe-48% Ni/P-7B actuators of $h_e = 0.2$ mm and $h_p = 0.1$, 0.2, and 0.4 mm. There appears to be negligible difference in the deflection for $h_p = 0.1$ mm and 0.2 mm. Figure 6 gives the plot of w_{tip} obtained from the beam theory as a function of h_p for the type a P-7B/Fe-48% Ni/P-7B actuator of $h_e = 0.2$ mm under $E_0 = 0.3$ MV/m. The tip deflection exhibits a maximum at $h_p \approx 0.13$ mm. Figure 7 shows the similar plot of w_{tip} versus h_e for $h_p = 0.2$ mm. Figure 8 shows the influence of the piezoelectric material properties and electric field E_0 on w_{tip} of the finite element solutions for $h_p = h_e = 0.2$ mm. The hyster-

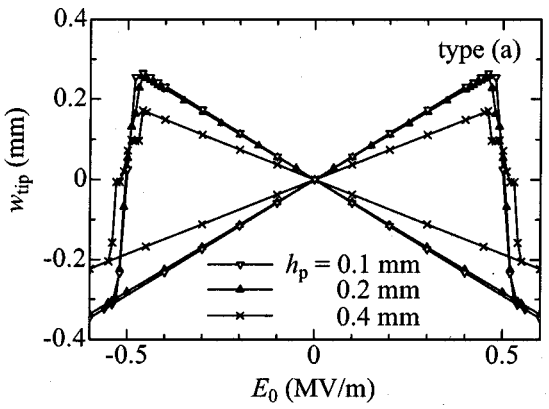

FIG. 5. Tip deflection vs electric field [P-7B, $h_e = 0.2$ mm, $(E_z)_1 = E_0$, and $(E_z)_3 = 0$].

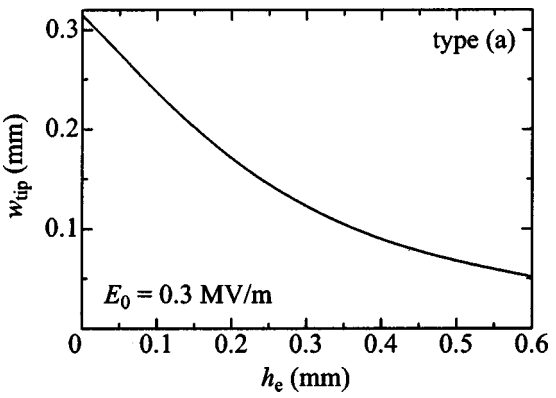

FIG. 7. Tip deflection vs elastic layer thickness [P-7B, $h_p = 0.2$ mm, $(E_z)_1 = E_0$, and $(E_z)_3 = 0$].

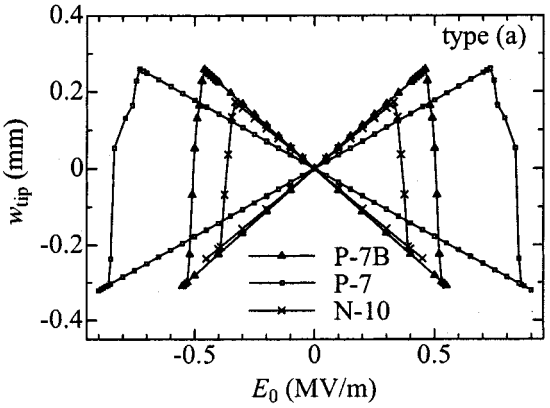

FIG. 8. Tip deflection vs electric field [$h_p = h_e = 0.2$ mm, $(E_z)_1 = E_0$, and $(E_z)_3 = 0$].

esis behaviors depend on the material of the laminated actuators.

VI. CONCLUSIONS

Laminated beam and 3D finite element analyses are presented for the cantilever piezoceramic/metal/piezoceramic actuator, in which the effects of electric fields and polarization switching are incorporated into the solutions of the displacement. The displacement of the cantilever piezoceramic/metal/piezoceramic actuator under the applied voltage is also measured. It has been demonstrated that the analytical predictions of the displacement and polarization switching properties are in excellent agreement with measured values. It has also been shown that the present analysis can be applied to piezoelectric laminated actuators with a wide range of piezoelectric material and geometrical properties. This study provides useful guidelines for the design of piezoelectric laminated actuators.

ACKNOWLEDGMENTS

This work was supported by the Ministry of Education, Culture, Sports, Science, and Technology of Japan under the Grant-in-Aid for Scientific Research (B) and Grant-in-Aid for Exploratory Research.

APPENDIX

For piezoceramics which exhibit symmetry of a hexagonal crystal of class 6 mm with respect to principal x_1, x_2, and x_3 axes, the constitutive relations can be written in the following form:

$$\begin{Bmatrix} \varepsilon_1 \\ \varepsilon_2 \\ \varepsilon_3 \\ \varepsilon_4 \\ \varepsilon_5 \\ \varepsilon_6 \end{Bmatrix} = \begin{bmatrix} s_{11} & s_{12} & s_{13} & 0 & 0 & 0 \\ s_{12} & s_{11} & s_{13} & 0 & 0 & 0 \\ s_{13} & s_{13} & s_{33} & 0 & 0 & 0 \\ 0 & 0 & 0 & s_{44} & 0 & 0 \\ 0 & 0 & 0 & 0 & s_{44} & 0 \\ 0 & 0 & 0 & 0 & 0 & s_{66} \end{bmatrix} \begin{Bmatrix} \sigma_1 \\ \sigma_2 \\ \sigma_3 \\ \sigma_4 \\ \sigma_5 \\ \sigma_6 \end{Bmatrix} + \begin{bmatrix} 0 & 0 & d_{31} \\ 0 & 0 & d_{31} \\ 0 & 0 & d_{33} \\ 0 & d_{15} & 0 \\ d_{15} & 0 & 0 \\ 0 & 0 & 0 \end{bmatrix} \begin{Bmatrix} E_1 \\ E_2 \\ E_3 \end{Bmatrix}, \tag{A1}$$

$$\begin{Bmatrix} D_1 \\ D_2 \\ D_3 \end{Bmatrix} = \begin{bmatrix} 0 & 0 & 0 & 0 & d_{15} & 0 \\ 0 & 0 & 0 & d_{15} & 0 & 0 \\ d_{31} & d_{31} & d_{33} & 0 & 0 & 0 \end{bmatrix} \begin{Bmatrix} \sigma_1 \\ \sigma_2 \\ \sigma_3 \\ \sigma_4 \\ \sigma_5 \\ \sigma_6 \end{Bmatrix} + \begin{bmatrix} \varepsilon_{11} & 0 & 0 \\ 0 & \varepsilon_{11} & 0 \\ 0 & 0 & \varepsilon_{33} \end{bmatrix} \begin{Bmatrix} E_1 \\ E_2 \\ E_3 \end{Bmatrix}, \tag{A2}$$

where

$$\left.\begin{array}{lll} \sigma_1 = \sigma_{11}, & \sigma_2 = \sigma_{22}, & \sigma_3 = \sigma_{33} \\ \sigma_4 = \sigma_{23} = \sigma_{32}, & \sigma_5 = \sigma_{31} = \sigma_{13}, & \sigma_6 = \sigma_{12} = \sigma_{21} \end{array}\right\}, \tag{A3}$$

$$\left.\begin{array}{lll} \varepsilon_1 = \varepsilon_{11}, & \varepsilon_2 = \varepsilon_{22}, & \varepsilon_3 = \varepsilon_{33} \\ \varepsilon_4 = 2\varepsilon_{23} = 2\varepsilon_{32}, & \varepsilon_5 = 2\varepsilon_{31} = 2\varepsilon_{13}, & \varepsilon_6 = 2\varepsilon_{12} = 2\varepsilon_{21} \end{array}\right\},$$

$$\left.\begin{array}{ll} s_{11} = s_{1111} = s_{2222}, & s_{12} = s_{1122}, \end{array}\right. \tag{A4}$$

$$\left.\begin{array}{ll} s_{13} = s_{1133} = s_{2233}, & s_{33} = s_{3333} \\ s_{44} = s_{2323} = s_{3131}, & s_{66} = s_{1212} = 2(s_{11} - s_{12}) \end{array}\right\}, \tag{A5}$$

$$d_{15} = 2d_{131} = 2d_{223}, \quad d_{31} = d_{311} = d_{322}, \quad d_{33} = d_{333}. \tag{A6}$$

[1] P. Donthireddy and K. Chandrashekhara, Comput. Struct. **35**, 237 (1996).
[2] S. A. Wise, Sens. Actuators A **69**, 33 (1998).
[3] X. Li, W. Y. Shih, I. A. Aksay, and W.-H. Shih, J. Am. Ceram. Soc. **82**, 1733 (1999).
[4] S. S. Vel and R. C. Batra, Smart Mater. Struct. **10**, 240 (2001).
[5] S. C. Hwang, C. S. Lynch, and R. M. McMeeking, Acta Metall. Mater. **43**, 2073 (1995).
[6] J. E. Huber and N. A. Fleck, J. Mech. Phys. Solids **49**, 785 (2001).
[7] Y. Shindo, W. Domon, and F. Narita, Arch. Mech. **49**, 403 (1997).
[8] Y. Shindo, W. Domon, and F. Narita, Theor. Appl. Fract. Mech. **28**, 175 (1998).
[9] Y. Shindo, M. Oka, and K. Horiguchi, ASME J. Eng. Mater. Technol. **123**, 293 (2001).
[10] Y. Shindo, H. Murakami, K. Horiguchi, and F. Narita, J. Am. Ceram. Soc. **85**, 1243 (2002).